Author Manuscript

Author Manuscript

Author Manuscript

Author Manuscript

HHS Public Access

Author manuscript

J Orthop Res. Author manuscript; available in PMC 2019 May 16.

Published in final edited form as:

J Orthop Res. 2016 August ; 34(8): 1418–1430. doi:10.1002/jor.23354.

In Vivo Measurement of Vertebral Endplate Surface Area along the Whole Spine

Maho Kishimoto[1], **Koji Akeda**[2], **Akihiro Sudo**[2], **Alejandro A. Espinoza Orías**[3], and **Nozomu Inoue**[3]

[1]Faculty of Medical and Life Sciences, Doshisha University, Kyoto, Japan

[2]Department of Orthopaedic Surgery, Mie University Graduate School of Medicine, Tsu City, Japan

[3]Department of Orthopedic Surgery, Rush University Medical Center, Chicago, IL, USA.

Abstract

Accurate determination of vertebral endplate surface area (SA) is crucial in spinal surgeries, implant design and sizing. However, the literature provides limited information on endplate SA along the entire human spine. Therefore, this study aims to contribute with baseline information on endplate SA in both genders using 3D-models of the superior and inferior endplates extracted from whole-spine myelogram computed-tomography (CT) data from 49 patients with spinal disorders. Endplate SA was measured by summation of unit-mesh element SA and projection onto a plane defined by the endplate normal vector. Individual endplate position was determined by the cumulative distance along the spinal column with respect to C2. Endplate area was analyzed by gender, spinal level and correlation with spinal position. Males had larger endplates than females at all levels ($p<0.05$) but S1. The inferior endplates were larger than their superior counterparts within the same vertebral body ($p<0.05$) at C3, C5, T1 through L2 and L4, respectively. For each intervertebral disc level, the cranial endplate was larger than the caudal endplate of the disc at the C5/C6, T1/T2 through T6/T7, T8/T9 and L4/L5 discs, while smaller at T11/T12, T12/L1 and L2/L3. There was a strong linear correlation between endplate area and spinal position in both genders ($r_{Males} = 0.938$ and $r_{Females} = 0.911$, respectively). SA was larger than the projected area by 12%, 4% and 4% in the cervical, thoracic and lumbar spines, respectively. To the best of the authors' knowledge, this is the first report of whole-spine endplate morphology measured *in vivo*.

Keywords

Endplate; Surface Area; Endplate geometry; Spine; Computed Tomography; Three-dimensional measurement

*Corresponding Author: Nozomu Inoue M.D., Ph.D., Department of Orthopedic Surgery, Rush University Medical Center, 1611 W Harrison Street, Suite 201 Orthopedic Building, Chicago, IL 60612, Nozomu_Inoue@rush.edu, Phone: 312-942-8151, Fax: 312-942-2040.

Authors' contribution statement:

Research design; acquisition, analysis or interpretation of data: MK, KA, AS, NI

Drafting of manuscript/Critical Review: MK, KA, NI, AEO

Approval of final version: All authors have read and approved the final submitted manuscript.

Author Manuscript Author Manuscript Author Manuscript Author Manuscript

INTRODUCTION

Accurate knowledge of vertebral endplate morphology is important to better understand its structure-function relationships,[1-4] with respect to its influence and role in intervertebral disc degeneration, and to design proper surgical procedures, tissue-engineered disc replacement constructs and spinal implants.[5; 6] Measurement of the endplate surface area provides essential information to be used for estimation of stress and pressure in intervertebral discs, estimation of disc volume and adequate sizing of spinal implants. To date, these endplate morphological parameters have been gathered mainly by means of planar methods.[6-13] However, since the endplate actually has a complex three-dimensional (3D) geometry, appropriate 3D endplate surface models are necessary for accurate measurements of any morphological parameter, including surface area. Information on the endplate surface area spanning the entire human spine is limited in the literature. To the best of the authors' knowledge, currently there is no *in vivo* study providing results of 3D-based endplate surface area measurements.

Continuous increases in endplate dimensions along the spine have been reported in the literature.[6, 7; 14; 15] We hypothesize that the endplate area increases as a function of distance from the C2 by increasing the size within the same vertebral body and/or between the endplates consisting of an intervertebral disc. The objective of this study was to contribute with baseline information on endplate areas of the whole-spine in both males and females using subject-based 3D whole-spine computed tomography (CT) models.

METHODS

Subjects

This IRB-approved study was conducted on 49 patients (male 25, female 24; range 22-88 years, average age 61.8 years old). The patients were suspected to have spinal stenosis and/or spinal cord disorders and confirmatory whole-spine CT myelographic measurements were ordered by the attending surgeon. The mean heights of the male and female patients were 165.1 ± 8.9 cm (mean ± SD) and 150.6 ± 7.2 cm, respectively. The mean weights of the male and female patients were 61.6 ± 12.7 kg and 56.7 ± 23.7 kg, respectively. The patients received whole-spine myelography CT imaging (tube voltage: 120 kV, tube current: 84.6 ± 11.8 mAs, pixel size: 0.39 ± 0.07 mm, field of view: 197.4 ± 33.3 mm, matrix: 512×512, slice increment: 1.0 mm, slice thickness: 1.0 mm), and were diagnosed as: lumbar spinal canal stenosis (n = 27), lumbar disc herniation (n = 14), cervical spondylosis (n = 3), cervical spondylotic radiculopathy (n = 2), cervical spondylotic myelopathy (n = 1), low back pain (n = 1) and lumbar disc disease (n = 1).

Creation of 3D Endplate Surface Models

CT images were reconstructed using a commercial 3D reconstruction software package (Mimics 16.0; Materialise Inc., Leuven, Belgium). Segmentation of each vertebra was performed using a threshold level of 226 Hounsfield Units and 3D whole-spine polygon-mesh models from C1 to S1 were created based on this data. The surface of the 3D polygon model was smoothed by using the "Wrap function" in the software package with the

Author Manuscript Author Manuscript Author Manuscript Author Manuscript

smallest detail level of 1.0 mm. Both superior and inferior endplates (relative to each vertebral body) were further segmented from each vertebral 3D model allowing for the creation of individual superior and inferior endplate polygon-mesh models. Whenever manifest cases of osteophytes were present, they were not included in the endplate model. A total of 2,352 endplate models were created from 1,176 vertebral bodies of C2 through S1 (Fig. 1).

Endplate Surface Area Measurements

For each endplate surface model, the mean normal vector was calculated by averaging the normal vectors of its individual mesh elements (Fig. 2). The angle between the mean normal vector and the normal vector of an individual polygon mesh element was calculated by means of the dot product and the polygon elements with a normal vector oriented less than 90° were included for area measurements. The following two methods were implemented to enable automatic endplate surface-area calculations using a custom-written routine in Microsoft Visual C++ under Microsoft Foundation Class (MFC) programming environment.

Polygon surface area measurement: The surface area of the endplate model was calculated by summation of individual polygon area through the entire surface of the endplate model.[7, 16] *Projected surface area measurement:* Each polygon element of the endplate mesh model was projected on a plane perpendicular to the mean normal vector of its corresponding endplate (Fig. 2). The projected surface area of the endplate was calculated by summation of individual polygon element projected surface area magnitudes.

Endplate Diameter Measurements and Endplate Area Calculation by Elliptical Approximation

In order to compare the endplate area with that estimated by a conventional method based on elliptical approximation, anteroposterior (AP) and transverse diameters were measured. Since the area by elliptical approximation is a planar area, the projected model was used for measurement of the diameters and the elliptical approximation area was compared with the projected area.

Anatomical axes and planes for individual endplate were determined by eigenvectors of each endplate using custom software. The most posterior point was determined in the midsagittal plane. The most anterior and the most lateral points of the model were determined based on the local anatomical axes. The AP diameter was determined by measuring the distances in space from the most posterior point to the coronal plane and from the most anterior point to the coronal plane using vector algebra. Similarly, the transverse diameter was determined by measuring the distances in space from the most lateral points for both sides to the sagittal plane using vector algebra. These procedures were used because the most anterior point and the most lateral points did not always exist on the sagittal plane or coronal plane, respectively. The endplate area was calculated using the AP and transverse diameters by elliptical approximation as follows: Elliptical approximation area (elliptical area) = AP diameter/2 x transverse diameter/2 x π.

Author Manuscript Author Manuscript Author Manuscript Author Manuscript

Determination of endplate position

In order to analyze the endplate as a function of distance from the inferior endplate of C2, the spinal position was determined as the sum of vertebral body height(s) and the intervening intervertebral disc height(s) towards the endplate of interest (Fig. 3).[7] The centroid of each endplate was located on the corresponding endplate point-cloud dataset model. The vertebral body height was determined by the distance between the centroids of superior and inferior endplates within the corresponding vertebral body. Similarly, the intervertebral disc height was determined by the distance between the centroid of inferior endplate in the cranial vertebral body and the centroid of the superior endplate of the caudal vertebral body. The distance to each endplate was normalized value by cranio-caudal distance (C2-S1) and presented as a percentage (%).

Statistical Analysis

Gender effects were compared with unpaired Student's *t*-tests. Level effects were sought by ANOVA with Fisher's PLSD *post hoc* tests using SPSS Statistics v. 23 (IBM, Armonk, NY). The superior vs. inferior endplate areas for each vertebral body, the superior vs. inferior endplate areas for each intervertebral disc, polygon surface area vs. projected area and the projected area vs. elliptical area were compared with paired Student's *t*-tests. Correlation between the endplate area vs. the spinal position was analyzed by simple linear regression analysis. Significance level was set at $p < 0.05$. Results are presented as mean ± SD.

RESULTS

Endplate polygon-mesh surface area:

The endplate polygon-mesh surface area was larger in males on both the superior and inferior endplates at all levels, with the exception of S1. The inferior endplate area was higher as compared with the superior endplate area within the same vertebral body at C3, C5, T1 through L2 and L4 (Fig. 4A). Within the intervertebral disc, the area of the inferior endplate of the cranial vertebral body (cranial endplate for the disc) was higher than the area of the superior endplate of the caudal vertebral body (caudal endplate for the disc) at the C5/C6, T1/T2 throughT6/T7, T8/T9 and L4/L5 discs, while lower at T11/T12, T12/L1 and L2/L3 (Fig. 4A). Strong linear correlations were found between the endplate area vs. the spinal length both in males and females with correlation coefficient values of $r = 0.938$ and $r = 0.911$, respectively (Fig. 5A, B).

The results of multiple comparisons among the spinal levels showed significant increases within 3 consecutive levels at C3 and T3-L2 levels in superior endplates and at C3, C5-C7 and T3-L2 levels in the inferior endplate in males, and at C3 and T4-L3 levels in the superior endplate and at C2, C6-C7 and T3-L3 levels in the inferior endplate in females (Fig. 6). Significant decreases were noted between L4 and L5 in the inferior endplate in both males and females (Fig. 6).

Endplate projected surface area:

The endplate projected area was larger in males on both the superior and inferior endplates at all levels aside from S1. The inferior endplate area was higher when compared against the

Author Manuscript Author Manuscript Author Manuscript Author Manuscript

superior endplate area within the same vertebral body at C3, C4, C5, T1 through L2 and L4, but lower at L5 (Fig. 4B). Within the intervertebral disc, the projected area of the inferior endplate of the cranial vertebral body (cranial endplate for the disc) was larger than with the areas of the superior endplate of the caudal vertebral body (caudal endplate for the disc) at the C2/C3, C4/C5, C7/T1 through T6/T7, T8/T9, L4/L5 and L5/S1 discs, while lower at T11/T12, T12/L1 and L2/L3. Strong linear correlations were found between the endplate area vs. the spinal distance both in males and females with correlation coefficient values of r = 0.943 and r =0.922, respectively (Fig. 5C, D).

The results of multiple comparisons among the spinal levels showed significant increases within 3 consecutive levels at C3, C4 and T3-L2 levels in superior endplates and at C2, C3, C6, C7 and T2-L2 levels in the inferior endplate in males, and at C3 and T4-L2 levels in the superior endplate and at C3, C6-C7 and T4-L2 levels in the inferior endplate in females (Fig. 6). Significant decreases were noted between L3-L5 vs. S1 in the superior endplate and between L3-L4 vs. L5 in the inferior endplate in males, and between L5 vs. S1 in the superior endplate and between L4 vs. L5 in the inferior endplate in females (Fig. 6).

Endplate polygon-mesh surface area vs. Endplate projected surface area;

The polygon-mesh surface area (3D surface) was larger than the projected area (planar surface) at all endplates. Overall, the polygon surface area/projected surface area ratio was 1.06 ± 0.05. When the results were segregated by cervical, thoracic and lumbar anatomical location, the ratios were 1.12 ± 0.06, 1.04 ± 0.03 and 1.04 ± 0.04, respectively. The mean ratios in the superior and inferior endplates were 1.07 ± 0.06 and 1.05 ± 0.04, respectively, and the mean ratio in the superior endplate was higher than that in the inferior endplate (Table 1).

The endplate projected surface area shows more significant differences, including: larger inferior than superior endplates within the same vertebral body at C4, smaller inferior than superior endplates within the same vertebral body at L5, larger inferior than superior endplates in the adjacent caudal vertebral body at the C2/C3, C4/C5 and C7/T1 disc levels, and smaller inferior than superior endplates in the adjacent caudal vertebral body at the L5/S1disc level, as compared with the polygon-mesh surface area.

Endplate AP diameter:

The endplate AP diameter was larger in males on both the superior and inferior endplates at all levels except superior endplate at L5. The inferior endplate AP diameter was higher as compared with the superior endplate AP diameter within the same vertebral body at C3 through T9, L1 and L4 (Fig. 7A). Within the intervertebral disc, the AP diameter of the inferior endplate of the cranial vertebral body (cranial endplate for the disc) was higher than the AP diameter of the superior endplate of the caudal vertebral body (caudal endplate for the disc) at the C2/C3 through T5/T6, L4/5 and L5/S1 discs, while lower at T10/T11 through L2/L3 (Fig. 7A).

The results of multiple comparisons among the spinal levels showed significant increases within 3 consecutive levels at C3, C5 and C7-T12 levels in superior endplates and at C2, C3, T1-T7 and T12-L3 levels in the inferior endplate in males, and at C3, C5 and T4-L2 levels in

Author Manuscript Author Manuscript Author Manuscript Author Manuscript

the superior endplate and at C2, C3 and C7-L1 levels in the inferior endplate in females (Fig. 8). Significant decreases were noted between L2-L4 vs. S1 and between L4 vs. L5 in the superior endplate in males, and between L5 vs. S1 in the superior endplate between and C5 vs. C7 and between L4 vs. L5 in the inferior endplate in females (Fig. 8).

Endplate transverse diameter:

The endplate transverse diameter was larger in males on both the superior and inferior endplates at all levels, with the exception of superior endplates of C3 through C6 and inferior endplates of C4 and C5. The inferior endplate transverse diameter was higher as compared with the superior endplate transverse diameter within the same vertebral body at C6 through L4 (Fig. 7B). Within the intervertebral disc, the transverse diameter of the inferior endplate of the cranial vertebral body (cranial endplate for the disc) was lower than the transverse diameter of the superior endplate of the caudal vertebral body (caudal endplate for the disc) at the C3/C4 through C7/T1 discs, while higher at T1/T11 through L1/L2 and L3/L4 through L5/S1 (Fig. 7B).

The results of multiple comparisons among the spinal levels showed significant increases within 3 consecutive levels at C3, C5 and C7-T12 levels in superior endplates and at C2, C3, T1-T7 and T12-L3 levels in the inferior endplate in males, and at C3, C5 and T4-L2 levels in the superior endplate and at C2, C3 and C7-L1 levels in the inferior endplate in females (Fig. 8). Significant decreases were noted between L2-L4 vs. S1 and between L4 vs. L5 in the superior endplate in males, and between L5 vs. S1 in the superior endplate between and C5 vs. C7 and between L4 vs. L5 in the inferior endplate in females (Fig. 8).

Endplate surface area by elliptical approximation:

The endplate surface area estimated by elliptical approximation using the AP and transverse diameters was smaller than the projected area (planar surface) at all endplates except L5 inferior endplates in both genders. Overall, the elliptical approximation area/projected surface area ratio was 0.92 ± 0.05. When the results were sub-divided by cervical, thoracic and lumbar anatomical location, the ratios were 0.93 ± 0.05, 0.93 ± 0.05 and 0.91 ± 0.05, respectively. The ratio was largest in the lumbar spine and followed by cervical spine and thoracic spine. The mean ratios in the superior and inferior endplates were 0.94 ± 0.05 and 0.91 ± 0.05, respectively, and the mean ratio in the inferior endplate was higher than that in the superior endplate (Table 2).

DISCUSSION

Although previous anthropological studies report linear dimensions for the vertebrae using cadaveric specimens [7-11; 13; 17], the present study is the first to measure *in vivo* 3D surface area of the bony endplates in humans along the entire spine. The present study measured 3D endplate surface area, projected endplate surface area as the cross-sectional area, which may have different clinical relevance. The results of the present study showed gender differences of the endplate surface area, in both polygon and projected areas, at all levels but S1. The inferior endplate projected surface area was larger compared with the superior endplate of the same vertebra except C6, C7, L3 and L5. When the superior and inferior endplates

Author Manuscript Author Manuscript Author Manuscript Author Manuscript

within the intervertebral disc were compared, the inferior endplate projected surface area of the cranial vertebra was larger than that in the superior endplate of the adjacent caudal vertebra excluding the C3/C4, C5/C6, C6/C7, T7/T8, T10/T11, L1/L2, L2/L3 and L3/4 disc levels. The endplate surface area increased linearly as a whole; however, there were regional specificities as described later.

The present study used two different methods to measure endplate surface area using subject-based 3D-CT whole-spine models. The polygon-mesh surface measurement determines the surface area of the endplates in spite of its complex 3D surface morphology. Since the 3D CT model is based on a polygon mesh, individual polygon surface measurement can be easily implemented (and extended to the entire surface model) once the proper segmentation of the endplate has been achieved. This method provides true surface area of the endplate which is relevant for studies involving the interface between the bony endplate and the intervertebral disc. However, when the cross-sectional area is of interest, the endplate area measured by summation of polygon-mesh surface may be overestimated due to concavity of the endplate and uncinate processes of the superior endplate at C3-T1. In fact, in the present study, the endplate area measured by polygon-mesh area measurement was always larger than the projected area especially in the cervical spine. The projected surface area represents the cross-sectional area and can be used for many purposes such as estimation of stress/pressure of the intervertebral disc and disc volume. Unlike projected area measurements using photographs of cadaveric specimens, the projected area measurement using the 3D model requires an additional procedure to define a reference plane in the model. In the present study, this procedure was done automatically by calculating the mean normal vector of the endplate to define orientation of the reference plane. It should be noted, however, that the polygon-based area measurement includes areas of small protrusions and dimples which may not be desirable for certain purposes. Especially, image-based polygon models potentially include rough surfaces due to image noise which causes overestimation of the surface area. Since we attempted to measure macroscopic surface area of the endplate in the present study, we eliminated surface structures that protruded or dipped less than 1.0 mm by surface smoothing considering voxel size used in this study. The endplate area estimated by elliptical approximation was about 92 % of the projected area and could be used as a simple method to calculate the endplate area. It should be noted however, that the elliptical area calculated in the present study used diameters measured in the plane in 3D space considering 3D orientation of the endplate. Therefore, when the axial CT images are used for measurement of the diameter, especially AP diameter, reduction of the diameter due to obliquity of the endplate should be considered for evaluation of the area by elliptical approximation.

The superior and inferior endplate areas linearly increased 5- to 6-fold from C2 to L4 regardless of the measurement methods, even though increases in area were of a small amount at each level. There are two possible mechanisms to increase the endplate area. One is to increase the endplate area within the same vertebral body; i.e. to increase the endplate area between the superior endplate and the inferior endplate. Another is to increase the endplate area within an intervertebral disc; i.e. to increase the endplate area between the inferior endplate of the cranial vertebral body and the superior endplate of the caudal vertebral body. As the results were summarized earlier, inferior endplate areas were larger

Author Manuscript Author Manuscript Author Manuscript Author Manuscript

than superior endplate areas in the same vertebral body in 17 disc levels for the polygon area and 18 disc levels for the projected area out of 23 disc levels. In comparison between the cranial and caudal endplates within an intervertebral disc, the areas of the cranial endplate (inferior endplate of the cranial vertebra) and the caudal endplate (superior endplate of the caudal vertebra), the cranial endplate of the disc was larger in 15 disc levels out of 23 disc levels studied in the present study. These findings indicate that an increase in endplate area is caused mainly by an increase in endplate area within each individual vertebral body. These results agree with a previous study which measured linear dimensions of cadaveric thoracic and lumbar spines in an attempt to characterize the so-called “vertebral wedging”. In said study, Masharawi *et al.* described that the trapezoidal shape of the vertebral body and an inverted trapezoidal shape of the disc space lend a “Chinese pagoda” shape to the thoracolumbar vertebral column (T1-L5).[15]

Although the endplate areas and diameters increased with the each consecutive lower spinal level as a whole, regional specificity was noted at several spinal levels. Significant decrease in the inferior endplate AP was shown between C5 and C7 in females. This finding may be explained by the existence of cervical enlargement of the spinal cord and larger vertebral body/spinal canal ratio in females.[18] Many of the parameters on endplate area and AP diameter lack statistical differences in the cervico-thoracic transitional region; however, the reason for this remains unexplained. Significant decreases in the transverse diameters were found at T4 in both superior and superior endplates in males and significant increases in superior and inferior endplates in both genders were found below the T4 level. The decrease in the transverse diameter towards T4 and the increase from T4 was highlighted in the aforementioned study by Masharawi et al. and this finding was discussed from evolutionary, kinematic and biomechanical aspects.[19-24] These sandglass-type changes in the transverse diameter may also be explained by influence of adjacent organs in the posterior mediastinum, especially arch of aorta and descending aorta. Interestingly, significant decreases in many parameters were also found at L5 and S1 levels in both genders, and this finding is consistent with previous cadaveric studies.[6; 8; 9; 12-15; 21] Higher stress is expected at the pelvic-lumbar junction as a base of the entire spinal column and therefore larger endplate area and dimensions are expected in this region from a biomechanical point of view. The reason of this finding is unclear; however, S1 consists of a pelvic inlet and adjacent pelvic organs and/or a fetus in the case of females, which may prevent increases in endplate area and dimensions at S1. Future studies will be required to clarify whether the endplate area in S1 satisfies the biomechanical demands or is sacrificed by anatomical constraints.

Strong linear correlations were found between the endplate area vs. the distance from the C2 inferior endplate both in males and females in the present study. This finding, together with the results of higher endplate area in males, may be due to larger body mass and more muscle forces experienced at each consecutive lower spinal level. Busscher *et al.* compared anatomical dimensions of whole-spine obtained from human and porcine cadavers.[7] In this study, while the endplate width and depth (anteroposterior length) increased from C3 to L5 in human, less increase in width and consistent depth were found in the porcine spine. These findings suggest that increase in endplate area as a function of the distance from C2 is more influenced by increasing body mass in the lower levels in the upright position in humans.

Author Manuscript Author Manuscript Author Manuscript Author Manuscript

Future studies comparing endplate areas of whole-spine of the human and quadrupeds using the same method will be required to test this hypothesis.

One of the limitations of the present study was that the subjects were patients with spinal disorders. The patients who showed primarily lumbar symptoms underwent whole-spine myelography CT for diagnosis of multilevel spinal stenosis; therefore, about 88% of the patients had lumbar disorders. Although noticeable osteophytes were excluded from the endplate area measurements, degenerative change may have affected the quantification of endplate area. Larger variation of the endplate area in the lumbar spine as compared with cervical and thoracic spines in the present study (Fig. 5) may be caused by the presence of lumbar disorders.

ACKNOWLEDGEMENT

This study was supported in part by NIH/NCCIH R01 AT006692.

REFERENCES

1. Hou Y, Luo Z. 2009 A study on the structural properties of the lumbar endplate: histological structure, the effect of bone density, and spinal level. Spine 34:E427–433. [PubMed: 19454994]
2. Noshchenko A, Plaseied A, Patel VV, et al. 2013 Correlation of vertebral strength topography with 3-dimensional computed tomographic structure. Spine 38:339–349. [PubMed: 22869060]
3. Lotz JC, Fields AJ, Liebenberg EC. 2013 The role of the vertebral end plate in low back pain. Global spine journal 3:153–164. [PubMed: 24436866]
4. Grant JP, Oxland TR, Dvorak MF. 2001 Mapping the structural properties of the lumbosacral vertebral endplates. Spine 26:889–896. [PubMed: 11317111]
5. Moore RJ. 2006 The vertebral endplate: disc degeneration, disc regeneration. European spine journal : official publication of the European Spine Society, the European Spinal Deformity Society, and the European Section of the Cervical Spine Research Society 15 Suppl 3:S333–337.
6. Wang Y, Battie MC, Videman T. 2012 A morphological study of lumbar vertebral endplates: radiographic, visual and digital measurements. European spine journal : official publication of the European Spine Society, the European Spinal Deformity Society, and the European Section of the Cervical Spine Research Society 21:2316–2323.
7. Busscher I, Ploegmakers JJ, Verkerke GJ, et al. 2010 Comparative anatomical dimensions of the complete human and porcine spine. European spine journal : official publication of the European Spine Society, the European Spinal Deformity Society, and the European Section of the Cervical Spine Research Society 19:1104–1114.
8. Chen H, Zhong J, Tan J, et al. 2013 Sagittal geometry of the middle and lower cervical endplates. European spine journal : official publication of the European Spine Society, the European Spinal Deformity Society, and the European Section of the Cervical Spine Research Society 22:1570–1575.
9. Frobin W, Brinckmann P, Biggemann M, et al. 1997 Precision measurement of disc height, vertebral height and sagittal plane displacement from lateral radiographic views of the lumbar spine. Clinical biomechanics (Bristol, Avon) 12 Suppl 1:S1–s63.
10. Lakshmanan P, Purushothaman B, Dvorak V, et al. 2012 Sagittal endplate morphology of the lower lumbar spine. European spine journal : official publication of the European Spine Society, the European Spinal Deformity Society, and the European Section of the Cervical Spine Research Society 21 Suppl 2:S160–164.
11. Mahato NK. 2011 Disc spaces, vertebral dimensions, and angle values at the lumbar region: a radioanatomical perspective in spines with L5-S1 transitions: clinical article. Journal of neurosurgery Spine 15:371–379. [PubMed: 21740126]

Author Manuscript Author Manuscript Author Manuscript Author Manuscript

12. Wang Y, Videman T, Battie MC. 2013 Morphometrics and lesions of vertebral end plates are associated with lumbar disc degeneration: evidence from cadaveric spines. The Journal of bone and joint surgery American volume 95:e26.
13. Zhou SH, McCarthy ID, McGregor AH, et al. 2000 Geometrical dimensions of the lower lumbar vertebrae--analysis of data from digitised CT images. European spine journal : official publication of the European Spine Society, the European Spinal Deformity Society, and the European Section of the Cervical Spine Research Society 9:242–248.
14. Chen H, Jiang D, Ou Y, et al. 2011 Geometry of thoracolumbar vertebral endplates of the human spine. European spine journal : official publication of the European Spine Society, the European Spinal Deformity Society, and the European Section of the Cervical Spine Research Society 20:1814–1820.
15. Masharawi Y, Salame K, Mirovsky Y, et al. 2008 Vertebral body shape variation in the thoracic and lumbar spine: characterization of its asymmetry and wedging. Clinical anatomy (New York, NY) 21:46–54.
16. Otsuka Y, An HS, Ochia RS, et al. 2010 In Vivo Measurement of Lumbar Facet Joint Area in Asymptomatic and Chronic Low Back Pain Subjects. Spine 35:924–928. [PubMed: 20354471]
17. Tan SH, Teo EC, Chua HC. 2004 Quantitative three-dimensional anatomy of cervical, thoracic and lumbar vertebrae of Chinese Singaporeans. European spine journal : official publication of the European Spine Society, the European Spinal Deformity Society, and the European Section of the Cervical Spine Research Society 13:137–146.
18. Hukuda S, Kojima Y 2002 Sex discrepancy in the canal/body ratio of the cervical spine implicating the prevalence of cervical myelopathy in men. Spine 27:250–253. [PubMed: 11805686]
19. Bastir M, Garcia Martinez D, Recheis W, et al. 2013 Differential growth and development of the upper and lower human thorax. PloS one 8:e75128. [PubMed: 24073239]
20. Garcia-Martinez D, Recheis W, Bastir M. 2016 Ontogeny of 3D rib curvature and its importance for the understanding of human thorax development. American journal of physical anthropology 159:423–431. [PubMed: 26890054]
21. Kunkel ME, Herkommer A, Reinehr M, et al. 2011 Morphometric analysis of the relationships between intervertebral disc and vertebral body heights: an anatomical and radiographic study of the human thoracic spine. Journal of anatomy 219:375–387. [PubMed: 21615399]
22. Plomp KA, Vietharsdottir US, Weston DA, et al. 2015 The ancestral shape hypothesis: an evolutionary explanation for the occurrence of intervertebral disc herniation in humans. BMC evolutionary biology 15:68. [PubMed: 25927934]
23. Whitcome KK. 2012 Functional implications of variation in lumbar vertebral count among hominins. Journal of human evolution 62:486–497. [PubMed: 22425070]
24. Wilke HJ, Geppert J, Kienle A. 2011 Biomechanical in vitro evaluation of the complete porcine spine in comparison with data of the human spine. European spine journal : official publication of the European Spine Society, the European Spinal Deformity Society, and the European Section of the Cervical Spine Research Society 20:1859–1868.

Author Manuscript Author Manuscript Author Manuscript Author Manuscript

CLINICAL SIGNIFICANCE

Information on the endplate area is essential to design spine devices such as artificial discs, interbody devices and their corresponding pre-operative planning. The footprint of these devices on endplate area is important to estimate load transmission through the device. The present study provided endplate areas both from the real 3D surface and the projected area corresponding to the cross sectional area throughout entire spine in different sites (inferior or superior endplates) and both genders. Current imaging techniques have allowed measurements of endplate polygon-mesh surface area using patient-specific 3D models but not the endplate cross sectional area. The 3D polygon surface area to projected surface area ratio provided by the present study allows estimation of relevant cross-sectional area using patient-specific imaging techniques. The present study also provided the data on relative position of the centroid of individual endplate as a distance from C2 which allows for calculation of intervertebral disc height and vertebral body height at each spinal level. These parameters, combined with the projected endplate area can be used for simple estimation of volumes of the intervertebral disc and vertebral body at any spinal levels from C2/C3 through L5/S1 and C3 through L5, respectively. A decrease in endplate area from L5 to S1 was found in the present study. This finding may be considered as a risk factor for disc degeneration at this spinal level; however, further investigation is necessary to explain the decrease in endplate area at this level.

Author Manuscript Author Manuscript Author Manuscript Author Manuscript

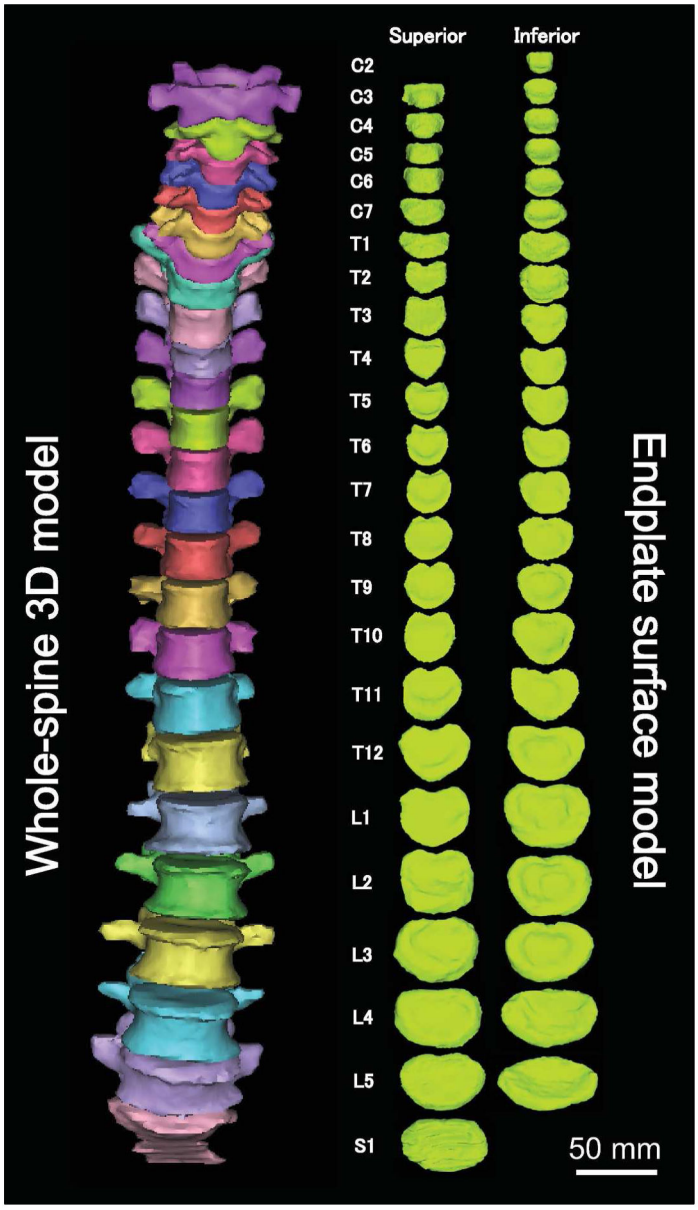

Fig. 1.
Whole-spine 3D model and endplate surface models.

Author Manuscript Author Manuscript Author Manuscript Author Manuscript

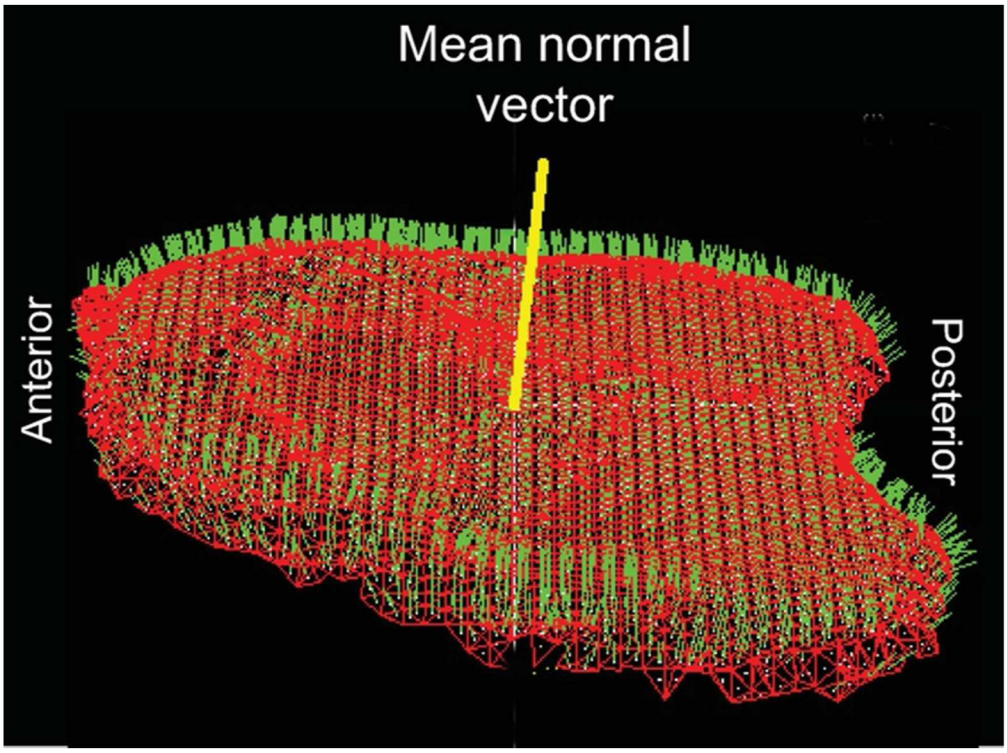

Fig. 2.

Endplate polygon-mesh model and the mean normal vector for the endplate surface model. Red lines: polygon element sides. Green lines: normal vector of individual polygon elements. Yellow line: mean normal vector.

Author Manuscript Author Manuscript Author Manuscript Author Manuscript

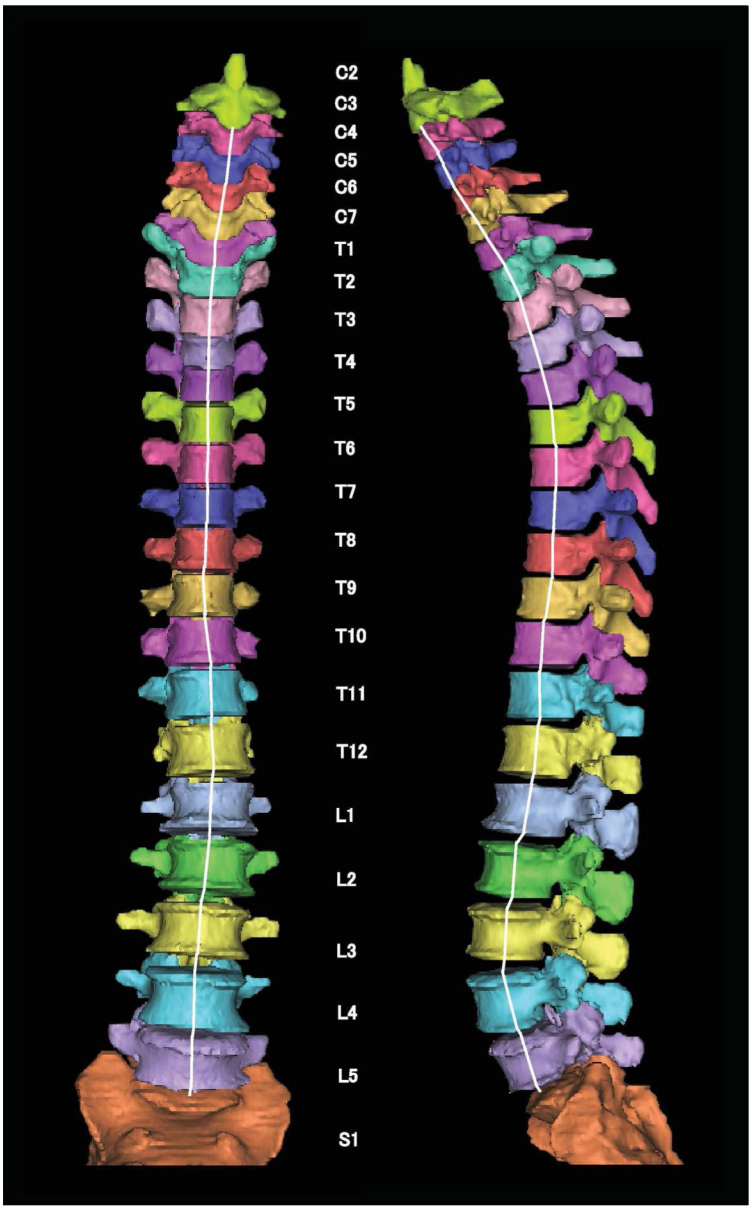

Fig. 3.

Spinal position determined by distance from centroid of the inferior C2 endplate. White lines show the cumulative distance path from the inferior endplate of C2 to the superior endplate of S1.

Author Manuscript Author Manuscript Author Manuscript Author Manuscript

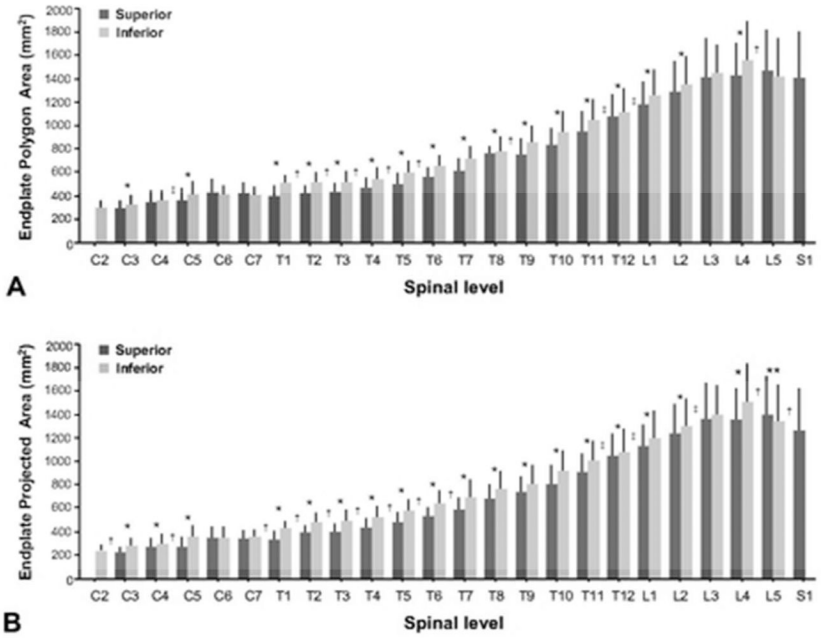

Fig. 4.

Endplate area by spinal level and anatomical site (superior or inferior). **A**: Endplate polygon area. **B**: Endplate projected area. *; Inferior > superior within a vertebral body ($p < 0.05$), † ; inferior of cranial vertebral body > superior of caudal vertebral body ($p < 05$), ‡ ; inferior of cranial vertebral body < superior of caudal vertebral body ($p < 0.05$) (mean ± SD).

Author Manuscript Author Manuscript Author Manuscript Author Manuscript

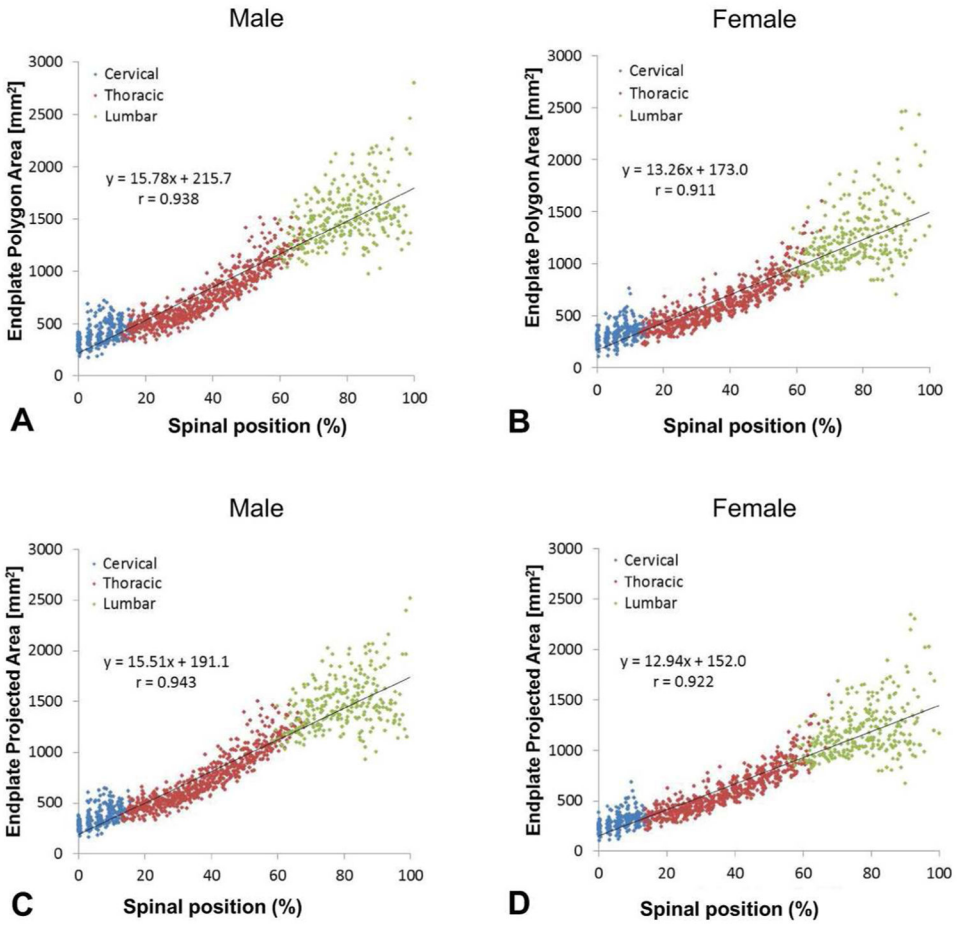

Fig. 5.

Correlations between endplate area and spinal length: **A**: endplate polygon area vs. spinal position in males. **B**: endplate polygon area vs. spinal position in females. **C**: endplate projected area vs. spinal position in males. **D**: endplate projected vs. spinal position in females.

Author Manuscript Author Manuscript Author Manuscript Author Manuscript

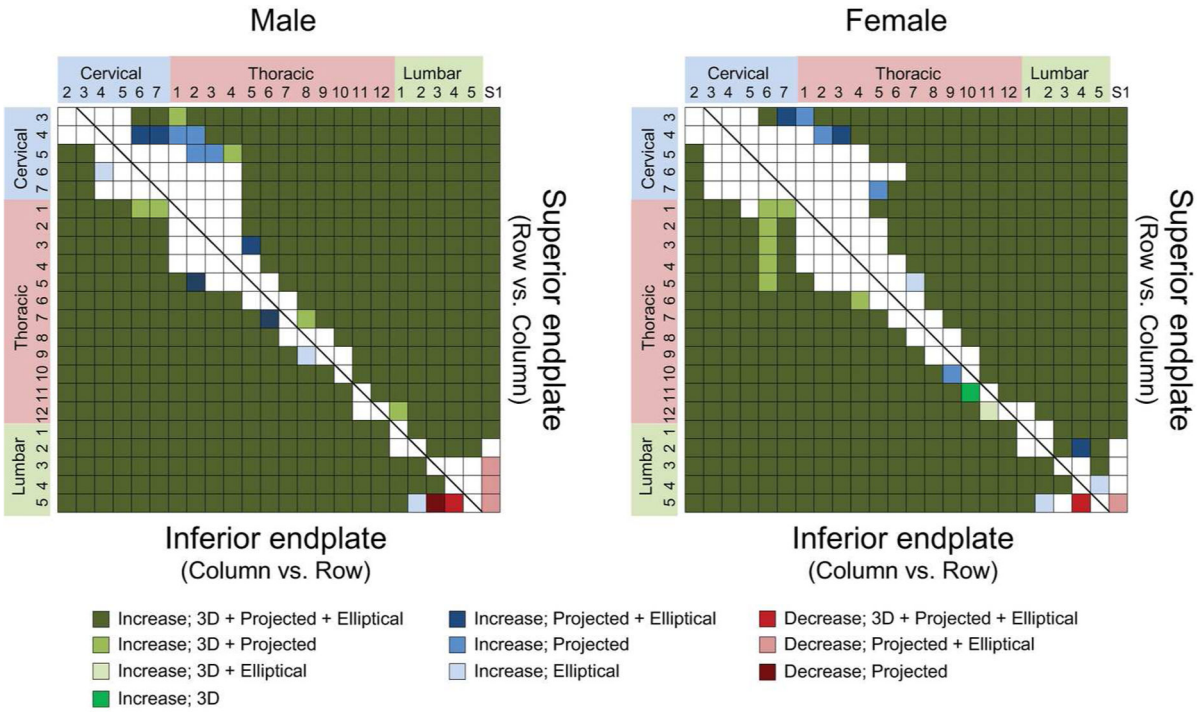

Fig. 6.

Results of multiple comparisons of endplate areas among the spinal levels by Fisher'sPLSD test ($p < 0.05$) by spinal level and anatomical site (superior or inferior). 3D: Endplate polygon surface area. Projected: Endplate projected area. Elliptical: Endplate surface area by elliptical approximation. The color of the matrix squares represents the largest change between column/row element pairs.

Author Manuscript
Author Manuscript
Author Manuscript
Author Manuscript

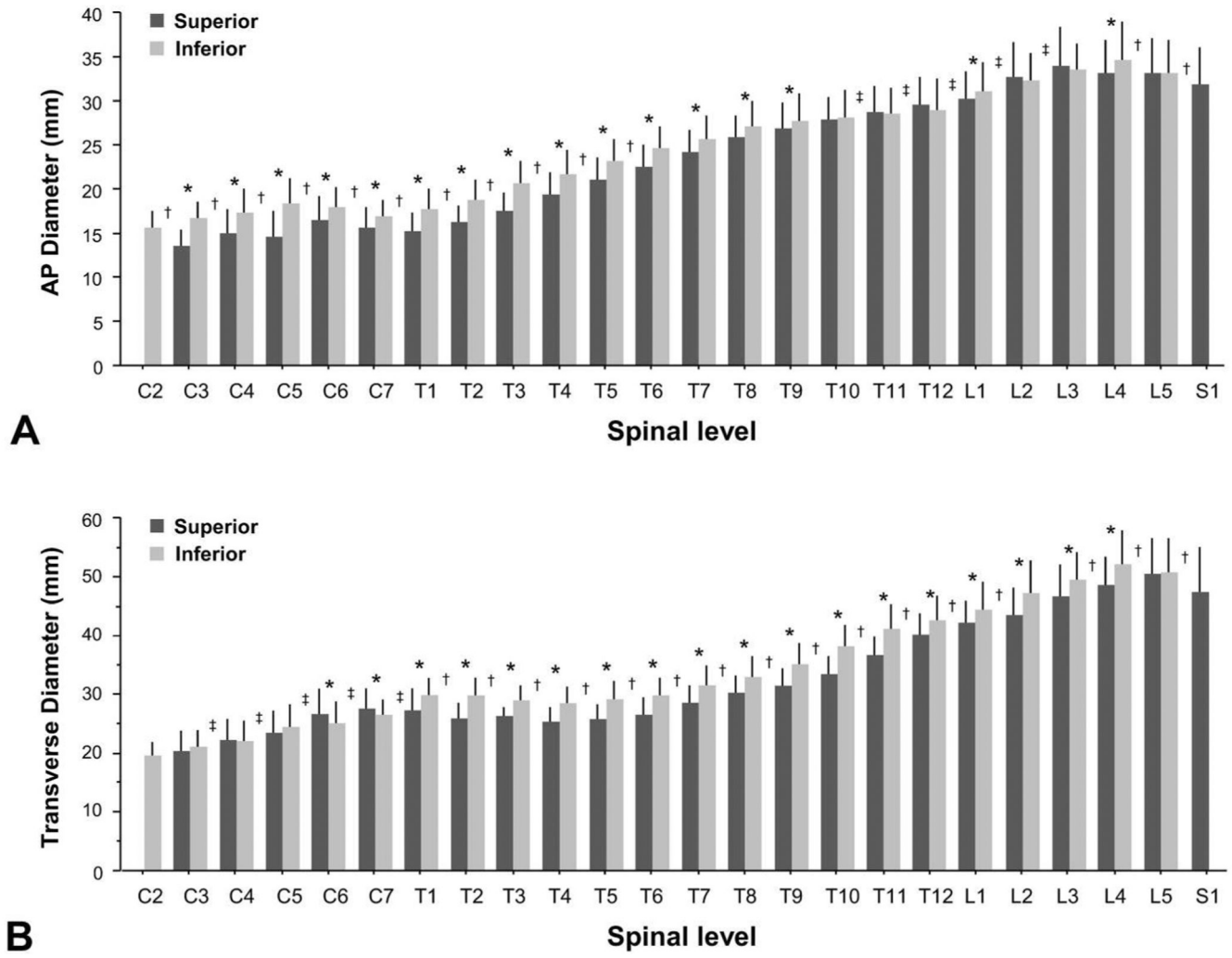

Fig. 7.

Endplate diameters by spinal level and anatomical position (superior or inferior). **A**: Anteroposterior (AP) diameter. **B**: Transverse diameter. * ; Inferior > superior within a vertebral body ($p<0.05$), ** ; Inferior < superior within a vertebral body ($p < 0.05$), † ; inferior of cranial vertebral body > superior of caudal vertebral body ($p < 0.05$), ‡ ; inferior of cranial vertebral body < superior of caudal vertebral body ($p < 0.05$) (mean ± SD).

Author Manuscript Author Manuscript Author Manuscript Author Manuscript

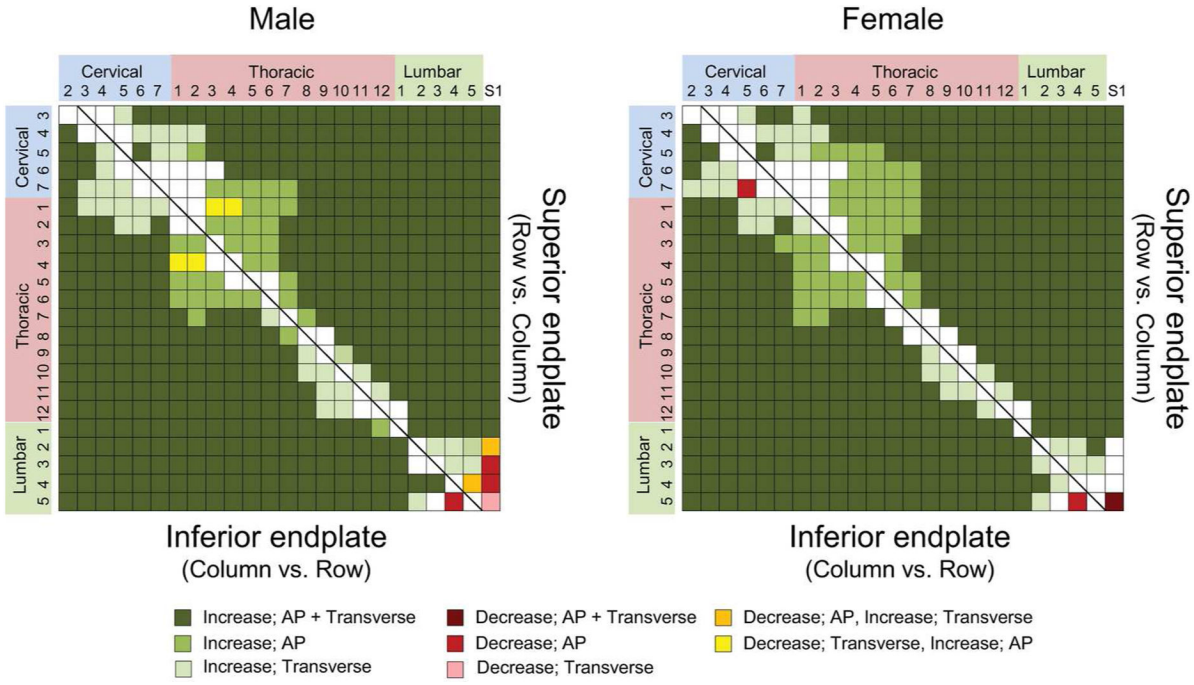

Fig. 8.

Results of multiple comparisons of endplate anteroposterior (AP) and transverse diameters among the spinal levels by Fisher's PLSD test ($p < 0.05$) by spinal level and anatomical site (superior or inferior). AP: AP diameter. Transverse: Transverse diameter. The color of the matrix squares represents the largest change between column/row element pairs.

Author Manuscript Author Manuscript Author Manuscript Author Manuscript

Table 1

Results for spine position, endplate polygon area, endplate projected area and polygon area/projected area ratio by spinal level, site and gender. Mean (SD)

Level	Site	Spinal position (mm)		Polygon-mesh surface area (mm^2)		Projected area (mm^2)		Polygon area/Projected area	
		Male	Female	Male	Female	Male	Female	Male	Female
C2	Inf	0.0	0.0	314.9 (55.1)	265.3 (52.3)	282.9 (44.3)	237.8 (43.8)	1.11 (0.06)	1.11 (0.05)
C3	Sup	3.3 (0.8)	2.7 (0.7)	307.7 (64.8)	265.0 (72.5)	259.2 (45.2)	224.6 (56.0)	1.18 (0.07)	1.17 (0.06)
	Inf	19.0 (1.2)	16.6 (1.3)	347.8 (74.1)	295.0 (71.8)	320.2 (61.1)	268.4 (57.4)	1.08 (0.04)	1.09 (0.04)
C4	Sup	22.0 (1.8)	19.4 (1.7)	376.9 (118.1)	303.3 (77.7)	324.1 (100.5)	258.9 (58.9)	1.16 (0.07)	1.16 (0.06)
	Inf	37.5 (2.6)	33.0 (2.5)	383.4 (88.8)	324.5 (75.4)	356.6 (79.9)	298.1 (68.8)	1.07 (0.04)	1.09 (0.02)
C5	Sup	40.6 (3.1)	35.5 (2.7)	394.9 (113.3)	320.3 (95.1)	337.8 (94.6)	273.0 (77.1)	1.17 (0.07)	1.17 (0.06)
	Inf	55.6 (4.0)	49.1 (3.1)	443.6 (94.9)	370.3 (115.7)	413.4 (86.6)	342.6 (104.6)	1.07 (0.04)	1.08 (0.03)
C6	Sup	58.6 (4.6)	51.3 (3.2)	469.0 (123.0)	390.4 (114.6)	414.3 (107.9)	340.9 (99.4)	1.13 (0.05)	1.15 (0.06)
	Inf	73.6 (5.7)	65.4 (4.2)	456.5 (62.6)	355.5 (75.8)	425.1 (58.0)	328.8 (72.0)	1.07 (0.04)	1.08 (0.03)
C7	Sup	76.7 (6.2)	68.4 (4.5)	465.0 (87.9)	364.2 (75.9)	416.6 (75.9)	324.7 (66.3)	1.12 (0.03)	1.12 (0.04)
	Inf	93.3 (7.1)	83.4 (5.5)	452.4 (64.8)	360.7 (53.0)	424.4 (64.1)	329.5 (47.2)	1.07 (0.03)	1.09 (0.03)
T1	Sup	96.7 (7.6)	86.9 (5.6)	441.3 (73.8)	348.6 (82.1)	404.4 (63.9)	314.7 (69.0)	1.09 (0.04)	1.10 (0.04)
	Inf	115.1 (8.5)	103.7 (6.5)	541.0 (62.4)	449.2 (74.4)	504.8 (58.8)	412.6 (67.0)	1.07 (0.02)	1.09 (0.03)
T2	Sup	118.9 (8.8)	106.9 (6.7)	458.4 (62.3)	369.0 (68.5)	423.7 (53.9)	340.8 (57.0)	1.08 (0.04)	1.08 (0.03)
	Inf	137.8 (9.6)	124.1 (7.5)	566.0 (59.2)	460.8 (72.4)	526.7 (52.3)	424.8 (64.9)	1.07 (0.03)	1.08 (0.02)
T3	Sup	141.2 (10.0)	127.3 (7.6)	467.0 (69.5)	380.9 (71.4)	434.9 (57.2)	355.5 (61.2)	1.07 (0.04)	1.07 (0.03)
	Inf	160.1 (10.7)	144.5 (8.5)	576.1 (62.3)	471.1 (78.5)	545.4 (59.6)	441.6 (70.8)	1.06 (0.02)	1.07 (0.03)
T4	Sup	163.4 (11.2)	147.6 (8.5)	509.9 (72.1)	410.2 (71.4)	481.4 (62.5)	384.7 (61.2)	1.06 (0.02)	1.06 (0.02)
	Inf	182.6 (11.9)	165.1 (9.4)	592.1 (77.8)	499.3 (97.5)	567.8 (74.0)	472.7 (86.5)	1.04 (0.02)	1.05 (0.02)
T5	Sup	185.8 (12.1)	168.1 (9.4)	552.4 (76.8)	450.9 (89.5)	529.3 (73.4)	428.0 (79.5)	1.04 (0.02)	1.05 (0.02)
	Inf	205.6 (12.8)	186.1 (10.4)	637.7 (88.9)	541.8 (108.4)	616.9 (83.9)	520.7 (99.8)	1.03 (0.02)	1.04 (0.02)
T6	Sup	208.7 (13.1)	189.0 (10.5)	603.8 (83.2)	491.2 (80.3)	583.4 (78.3)	470.7 (69.7)	1.03 (0.02)	1.04 (0.02)
	Inf	229.2 (13.6)	207.3 (11.7)	702.7 (88.6)	590.7 (89.2)	686.2 (88.1)	572.3 (81.3)	1.02 (0.01)	1.03 (0.02)
T7	Sup	232.2 (13.7)	210.3 (11.9)	675.4 (83.3)	556.7 (84.4)	661.1 (83.5)	540.0 (76.7)	1.02 (0.01)	1.03 (0.02)
	Inf	253.0 (14.4)	229.1 (12.9)	777.7 (105.4)	638.1 (98.6)	764.9 (105.8)	621.6 (91.1)	1.02 (0.01)	1.03 (0.02)
T8	Sup	256.6 (14.5)	232.5 (13.2)	772.8 (108.9)	627.2 (91.7)	755.7 (105.9)	606.3 (83.8)	1.02 (0.01)	1.03 (0.03)
	Inf	277.6 (15.0)	251.8 (13.9)	859.4 (110.4)	683.1 (123.1)	844.6 (108.2)	663.9 (112.2)	1.02 (0.01)	1.03 (0.02)
T9	Sup	281.5 (15.2)	255.3 (14.0)	842.4 (112.0)	660.4 (100.2)	824.2 (110.5)	642.3 (94.6)	1.02 (0.01)	1.03 (0.02)
	Inf	303.3 (15.9)	275.0 (15.0)	936.8 (110.9)	738.7 (106.8)	917.1 (109.4)	719.9 (101.9)	1.02 (0.01)	1.03 (0.02)
T10	Sup	307.5 (16.1)	278.5 (15.4)	919.9 (111.6)	733.9 (97.3)	901.6 (109.0)	715.1 (90.2)	1.02 (0.01)	1.03 (0.02)
	Inf	330.4 (17.0)	299.5 (16.4)	1052.7 (152.2)	835.5 (131.4)	1030.8 (150.5)	816.6 (125.7)	1.02 (0.01)	1.02 (0.02)
T11	Sup	335.4 (17.4)	303.8 (16.5)	1047.2 (855.1)	855.1 (136.0)	1025.9 (126.8)	832.8 (126.5)	1.02 (0.01)	1.03 (0.02)
	Inf	359.7 (18.5)	326.2 (17.7)	1163.0 (157.4)	908.1 (157.2)	1140.0 (150.1)	887.5 (153.3)	1.02 (0.01)	1.02 (0.02)
T12	Sup	365.2 (18.9)	331.2 (17.6)	1178.2 (147.3)	965.7 (170.0)	1159.5 (142.8)	944.4 (162.9)	1.02 (0.01)	1.02 (0.01)
	Inf	391.3 (20.2)	355.4 (18.8)	1220.7 (126.6)	995.5 (189.8)	1193.2 (123.6)	966.4 (182.1)	1.02 (0.01)	1.03 (0.02)
L1	Sup	397.5 (20.3)	361.2 (19.0)	1280.1 (153.6)	1056.2 (191.5)	1252.2 (144.9)	1023.3 (170.0)	1.02 (0.01)	1.03 (0.03)

Author Manuscript

Author Manuscript

Author Manuscript

Author Manuscript

Level	Site	Spinal position (mm)		Polygon-mesh surface area (mm^2)		Projected area (mm^2)		Polygon area/Projected area	
		Male	Female	Male	Female	Male	Female	Male	Female
	Inf	424.7 (21.4)	385.9 (20.6)	1371.9 (172.6)	1143.4 (218.0)	1340.2 (166.2)	1106.4 (203.8)	1.02 (0.01)	1.03 (0.02)
L2	Sup	432.4 (21.7)	393.0 (20.6)	1447.3 (191.6)	1124.4 (213.5)	1410.2 (179.6)	1096.2 (199.9)	1.03 (0.02)	1.02 (0.01)
	Inf	459.9 (22.9)	419.2 (21.8)	1493.6 (198.6)	1195.3 (201.9)	1457.6 (193.4)	1160.9 (185.8)	1.02 (0.01)	1.03 (0.02)
L3	Sup	468.8 (23.4)	426.8 (21.7)	1582.4 (271.0)	1246.8 (261.2)	1539.3 (252.2)	1202.2 (219.0)	1.03 (0.02)	1.03 (0.03)
	Inf	496.7 (24.7)	452.9 (23.4)	1592.4 (213.6)	1291.4 (183.6)	1551.2 (204.3)	1248.9 (167.6)	1.03 (0.01)	1.03 (0.02)
L4	Sup	505.4 (24.3)	460.9 (23.9)	1581.9 (216.4)	1273.8 (251.3)	1528.4 (204.6)	1223.5 (218.6)	1.03 (0.02)	1.04 (0.03)
	Inf	532.9 (25.7)	486.8 (25.2)	1699.8 (283.0)	1408.0 (325.7)	1641.5 (257.4)	1356.4 (306.5)	1.03 (0.02)	1.04 (0.02)
L5	Sup	540.9 (25.8)	494.0 (24.9)	1579.1 (251.7)	1357.7 (402.3)	1504.4 (223.5)	1292.4 (370.9)	1.05 (0.03)	1.05 (0.02)
	Inf	567.5 (27.3)	518.8 (26.2)	1560.7 (283.9)	1272.8 (294.6)	1476.5 (263.8)	1203.7 (269.6)	1.06 (0.03)	1.06 (0.02)
S1	Sup	575.4 (27.5)	526.2 (26.3)	1505.4 (372.4)	1303.4 (413.7)	1371.2 (322.4)	1157.0 (330.3)	1.10 (0.05)	1.12 (0.07)

Abbreviations: Sup: superior endplate, Inf: inferior endplate.

Author Manuscript Author Manuscript Author Manuscript Author Manuscript

Table 2

Antero-posterior (AP) diameter, transverse diameter, endplate area by elliptical approximation and elliptical area/projected area ratio by spinal level, site and gender. Mean (SD)

Level	Site	AP diameter (mm)		Transverse diameter (mm)		Elliptical area (mm^2)		Elliptical area/Projected area	
		Male	Female	Male	Female	Male	Female	Male	Female
C2	Inf	16.5 (2.1)	14.7 (1.1)	20.2 (2.2)	18.5 (2.7)	262.7 (5.14)	214.6 (40.1)	0.939 (0.065)	0.903 (0.051)
C3	Sup	14.3 (1.6)	12.9 (1.8)	20.7 (2.9)	20.1 (3.6)	232.8 (44.5)	207.3 (57.3)	0.913 (0.053)	0.920 (0.056)
	Inf	17.5 (2.0)	15.7 (1.6)	21.9 (2.4)	20.0 (2.7)	302.1 (58.1)	249.2 (57.3)	0.960 (0.059)	0.926 (0.040)
C4	Sup	15.8 (3.1)	14.0 (1.9)	23.1 (4.0)	21.3 (3.1)	292.9 (103.8)	235.7 (57.3)	0.914 (0.045)	0.910 (0.042)
	Inf	18.3 (2.4)	16.3 (2.3)	22.4 (3.7)	21.5 (3.0)	324.3 (82.4)	279.7 (78.1)	0.921 (0.055)	0.932 (0.053)
C5	Sup	15.8 (2.9)	13.3 (2.1)	24.1 (3.5)	22.7 (3.6)	303.9 (95.8)	241.6 (72.1)	0.911 (0.043)	0.885 (0.049)
	Inf	19.5 (2.7)	17.2 (2.4)	25.1 (3.7)	23.4 (4.6)	386.8 (88.3)	321.5 (110.1)	0.949 (0.052)	0.932 (0.049)
C6	Sup	17.5 (2.7)	15.2 (2.5)	27.4 (4.5)	25.7 (4.2)	381.8 (110.7)	311.3 (95.1)	0.930 (0.048)	0.912 (0.049)
	Inf	19.3 (1.8)	16.5 (1.6)	26.4 (2.8)	23.6 (3.9)	401.5 (61.4)	308.8 (78.1)	0.958 (0.041)	0.935 (0.057)
C7	Sup	16.8 (2.2)	14.4 (1.5)	28.8 (3.1)	26.0 (3.4)	380.2 (71.3)	296.0 (66.5)	0.929 (0.036)	0.909 (0.047)
	Inf	18.2 (1.4)	15.7 (1.2)	27.6 (2.6)	24.9 (2.2)	395.6 (57.5)	308.2 (46.4)	0.948 (0.045)	0.934 (0.044)
T1	Sup	16.3 (1.7)	14.0 (1.8)	28.5 (3.1)	25.7 (3.7)	365.2 (61.7)	284.6 (68.3)	0.916 (0.055)	0.900 (0.036)
	Inf	18.8 (1.8)	16.6 (2.0)	31.3 (2.2)	28.7 (2.5)	462.2 (61.3)	375.3 (71.7)	0.929 (0.030)	0.907 (0.047)
T2	Sup	16.9 (1.6)	15.4 (2.1)	26.9 (2.7)	24.6 (2.2)	356.3 (46.3)	297.4 (59.0)	0.855 (0.045)	0.872 (0.074)
	Inf	19.7 (2.3)	17.7 (2.0)	31.8 (2.0)	28.3 (2.6)	492.4 (66.1)	394.0 (67.4)	0.947 (0.055)	0.926 (0.047)
T3	Sup	18.4 (1.8)	16.4 (2.0)	26.3 (2.5)	24.2 (2.2)	381.8 (54.8)	312.5 (56.0)	0.891 (0.047)	0.879 (0.038)
	Inf	21.7 (2.3)	19.3 (2.1)	30.7 (2.1)	26.9 (2.1)	523.1 (62.2)	409.7 (67.4)	0.974 (0.044)	0.928 (0.049)
T4	Sup	20.6 (2.2)	18.2 (2.2)	26.5 (2.2)	23.8 (1.9)	428.2 (55.2)	342.0 (58.6)	0.905 (0.050)	0.889 (0.040)
	Inf	23.0 (2.3)	20.3 (2.3)	29.5 (2.1)	27.3 (3.1)	533.7 (69.9)	438.5 (89.6)	0.956 (0.048)	0.926 (0.057)
T5	Sup	22.4 (2.0)	19.7 (2.2)	26.8 (2.0)	24.5 (2.0)	473.1 (62.9)	379.9 (65.1)	0.910 (0.046)	0.890 (0.041)
	Inf	24.3 (2.2)	22.0 (2.2)	30.5 (2.6)	27.3 (2.8)	583.6 (75.2)	474.6 (89.2)	0.963 (0.050)	0.913 (0.037)
T6	Sup	23.8 (2.2)	21.3 (1.9)	28.1 (2.5)	25.1 (2.2)	526.1 (75.0)	421.1 (65.9)	0.916 (0.048)	0.895 (0.042)
	Inf	25.8 (2.2)	23.4 (2.0)	31.4 (2.5)	28.1 (2.4)	637.3 (83.4)	517.9 (76.6)	0.945 (0.046)	0.906 (0.041)
T7	Sup	25.5 (2.0)	22.9 (2.0)	30.0 (2.6)	26.5 (2.0)	600.8 (79.9)	477.7 (70.7)	0.924 (0.042)	0.885 (0.031)
	Inf	27.2 (2.5)	24.1 (2.0)	33.2 (2.8)	29.6 (2.5)	710.6 (107.4)	561.9 (81.5)	0.943 (0.039)	0.905 (0.033)
T8	Sup	27.2 (2.3)	24.3 (1.8)	31.7 (2.8)	28.4 (2.4)	679.3 (105.9)	543.0 (74.9)	0.913 (0.054)	0.897 (0.034)
	Inf	28.6 (2.4)	25.3 (2.5)	34.8 (3.2)	30.8 (2.7)	782.9 (112.5)	615.8 (100.5)	0.941 (0.049)	0.929 (0.038)
T9	Sup	28.6 (2.6)	25.0 (2.0)	32.9 (2.9)	29.7 (2.5)	742.3 (118.1)	584.3 (84.9)	0.914 (0.049)	0.911 (0.046)
	Inf	29.6 (2.6)	25.7 (2.1)	37.1 (2.9)	33.0 (2.9)	862.9 (115.9)	668.2 (103.4)	0.955 (0.037)	0.928 (0.029)
T10	Sup	29.5 (2.2)	26.1 (1.7)	34.9 (3.1)	31.1 (2.8)	811.4 (116.7)	638.0 (84.5)	0.913 (0.045)	0.907 (0.033)
	Inf	29.9 (2.6)	26.3 (2.3)	40.1 (3.4)	35.7 (3.1)	946.1 (149.5)	741.1 (122.8)	0.932 (0.039)	0.893 (0.042)
T11	Sup	30.2 (2.5)	27.1 (2.6)	38.2 (2.5)	34.7 (3.0)	909.1 (119.6)	742.1 (126.4)	0.900 (0.034)	0.890 (0.035)
	Inf	30.0 (2.5)	26.8 (2.6)	43.7 (3.2)	37.8 (3.7)	1034.4 (141.8)	800.3 (148.7)	0.922 (0.034)	0.901 (0.030)
T12	Sup	31.2 (2.5)	27.9 (2.7)	42.2 (3.2)	37.7 (3.2)	1037.2 (143.9)	830.4 (148.4)	0.908 (0.041)	0.880 (0.037)
	Inf	30.1 (2.4)	27.8 (3.9)	45.3 (2.4)	40.0 (3.9)	1073.0 (117.0)	881.6 (211.6)	0.914 (0.034)	0.908 (0.075)
L1	Sup	31.5 (2.5)	28.9 (3.0)	43.8 (3.2)	39.8 (3.7)	1087.8 (147.7)	908.8 (176.0)	0.881 (0.031)	0.886 (0.033)
	Inf	32.3 (2.9)	29.8 (3.1)	47.0 (3.3)	42.3 (4.3)	1195.6 (170.7)	996.4 (203.2)	0.911 (0.044)	0.899 (0.030)

Author Manuscript

Author Manuscript

Author Manuscript

Author Manuscript

Level	Site	AP diameter (mm)		Transverse diameter (mm)		Elliptical area (mm^2)		Elliptical area/Projected area	
		Male	Female	Male	Female	Male	Female	Male	Female
L2	Sup	34.8 (3.2)	30.5 (3.4)	46.3 (3.4)	40.5 (3.7)	1268.1 (195.9)	978.9 (196.8)	0.911 (0.038)	0.891 (0.036)
	Inf	33.8 (2.5)	30.8 (2.8)	50.5 (4.9)	43.8 (3.8)	1344.4 (197.0)	1064.3 (185.2)	0.937 (0.034)	0.916 (0.030)
L3	Sup	36.0 (4.2)	31.9 (3.2)	49.7 (4.5)	43.2 (4.3)	1414.7 (265.0)	1087.7 (216.1)	0.931 (0.037)	0.904 (0.034)
	Inf	34.7 (2.9)	32.2 (2.5)	52.2 (3.7)	46.5 (4.0)	1427.8 (194.7)	1179.1 (181.0)	0.935 (0.034)	0.942 (0.032)
L4	Sup	34.8 (3.5)	31.4 (3.3)	51.2 (3.5)	45.4 (4.9)	1406.1 (210.5)	1128.4 (233.6)	0.934 (0.035)	0.919 (0.035)
	Inf	36.2 (3.6)	33.1 (4.2)	54.9 (4.6)	49.6 (5.5)	1566.8 (262.2)	1304.9 (316.4)	0.969 (0.038)	0.960 (0.030)
L5	Sup	34.0 (3.0)	32.3 (4.2)	52.8 (3.8)	47.6 (7.0)	1416.9 (211.0)	1226.4 (363.5)	0.957 (0.032)	0.948 (0.031)
	Inf	34.6 (3.0)	31.5 (3.7)	53.4 (4.5)	48.0 (5.9)	1461.7 (252.4)	1201.2 (283.7)	1.007 (0.037)	0.997 (0.045)
S1	Sup	33.2 (4.1)	30.6 (3.5)	49.9 (6.3)	44.9 (8.0)	1316.9 (327.3)	1096.5 (312.6)	0.972 (0.048)	0.942 (0.032)

Abbreviations: Sup: superior endplate, Inf: inferior endplate, AP diameter: anterior-posterior diameter at mid-sagittal plane, Elliptical area = (AP diameter/2) × (transverse diameter/2) × π